JOURNAL OF GUIDANCE, CONTROL, AND DYNAMICS
Vol. 30, No. 5, September–October 2007

Separation Analysis Methodology for Designing Area Navigation Arrival Procedures

Liling Ren* and John-Paul B. Clarke†
Georgia Institute of Technology, Atlanta, Georgia 30332-0150

DOI: 10.2514/1.27067

The full benefits of Area Navigation arrival procedures are achieved when they are performed without interruption. However, current separation minima or miles-in-trail restrictions at terminal area boundaries are not sufficiently large in many instances to ensure uninterrupted execution of Area Navigation arrivals, and air traffic controllers have to frequently vector aircraft off the Area Navigation procedure to maintain separation. We present a theoretical framework, a separation analysis methodology, and a Monte Carlo Tool for the Analysis of Separation and Throughput (TASAT), which may be used to determine the target spacing at a selected intermediate metering point such that there is a desired probability that the procedure can be completed without controller intervention. TASAT includes stochastic models of various uncertainty factors such as pilot actions, aircraft weight, and winds. Numeric simulation and separation analyses were performed for a hypothetical Area Navigation arrival procedure to demonstrate the applicability of the methodology, and to investigate the relationship between target spacing, probability of uninterrupted procedure execution, and traffic throughput. Sensitivity analyses were also performed on the location of the metering point and different winds.

I. Introduction

AIRCRAFT with Area Navigation (RNAV) capability are able to navigate through the air on preplanned trajectories that do not cause them to exceed their performance and safety limits. These trajectories are defined by a series of waypoints that are not necessarily designated by conventional radio navigation aids. Corresponding altitude and speed constraints may also be given at waypoints. The waypoints define the desired lateral path, whereas the altitude and speed constraints jointly define the desired vertical path and speed profile.

The many benefits of RNAV terminal area procedures have been documented in previous studies [1,2]. Specific to RNAV arrival procedures, these benefits include improved pilots' and controllers' situation awareness and safety, reduced air-ground communication, reduced flight time and distance, reduced dispersion of flight times and distance, and reduced fuel burn. A special class of RNAV arrival procedures with optimized vertical profiles, the continuous descent arrival (CDA), has been proven to significantly reduce community noise impact and emissions in addition to the aforementioned benefits [3–5]. With these benefits in mind, the FAA has made expanded RNAV procedure implementation a higher priority [6].

Although RNAV procedures have been used extensively in the enroute environment for many years, their use in the terminal area has been limited. This is due in part to the continued use of vectoring for sequencing and spacing, and the inconsistency of this practice with a form of navigation that requires preprogrammed objectives (lateral and vertical flight paths). For example, although approximately 90% of the traffic at Las Vegas McCarran International Airport (KLAS) are RNAV capable, many of the RNAV-equipped aircraft that filed for an RNAV procedure were vectored for sequencing and spacing [7].

One factor driving the need for vectoring, and the resulting loss of RNAV benefits, is that the spacing at the point where aircraft are handed off from the Air Route Traffic Control Center (CENTER) to the Terminal Radar Approach Control (TRACON) is often not sufficient for the RNAV procedures to be executed without Air Traffic Control (ATC) intervention. Proposed solutions include long-term ones such as airborne precision spacing [8], and near-term improvements to vectoring techniques such as reductions in the use of heading vectoring, increased reliance on speed adjustments, and the use of lateral offsets [9].

In this paper, an alternative near-term operational concept is presented. In this concept, the need for controller intervention during RNAV arrivals is reduced to a minimum for any given traffic condition. Target spacings, which allow for uninterrupted operation of RNAV arrival procedures with certain probability, are recommended for a specified metering point based on rigorous theoretical and numerical analyses. No new capability is required onboard the aircraft. The benefits of this concept come from moving some of the spacing efforts to higher altitudes where aircraft are more efficient and farther from the ground.

The remainder of this paper is organized as follows: A conceptual framework for RNAV arrival procedures is presented in the next section. This is followed by a theoretical discussion of the separation analysis methodology that has been developed, and a brief description of the Monte Carlo simulation tool that has also been developed to support the application of the separation analysis methodology. A simulation study is then presented to demonstrate the application of the conceptual framework and the separation analysis methodology. The major findings of this research are summarized in the last section.

II. Conceptual Framework

A. Conventional Arrival and Approach Procedures

In a conventional arrival and approach, controllers orchestrate the movement of aircraft and achieve the desired sequencing and spacing on the final approach through vectoring: the process of giving pilots ad hoc altitude, speed, and heading commands. The primary benefit of vectoring is that it gives controllers the flexibility that has, to date, been required to achieve a tightly spaced final approach queue, thereby maximizing runway throughput, which is essential to minimizing delays when there is high traffic demand. However, vectoring is most frequently conducted at low altitude, resulting in flight time, noise, emissions, and fuel burn values that are significantly higher than their respective minimum possible values [3–5]. As seen in Fig. 1, the number of heading changes is significant,

Received 5 August 2006; revision received 22 January 2007; accepted for publication 22 January 2007.

*Research Engineer, Daniel Guggenheim School of Aerospace Engineering, 270 Ferst Drive NW. Senior Member AIAA.

†Associate Professor, Daniel Guggenheim School of Aerospace Engineering, 270 Ferst Drive NW. Associate Fellow AIAA.

as is flight distance and the extent to which flight tracks span the area around the airport. If this variation could be reduced, controller-pilot communication and flight time could be significantly reduced, as could the size of noise contours, the amount of emissions, and fuel burn.

B. RNAV Arrival Procedures

The lateral flight path of an RNAV arrival is defined by a series of waypoints. The flight management system (FMS), coupled with the autopilot, guide the aircraft along the preprogrammed lateral path. RNAV arrivals may terminate at a point outside of the coverage area of the instrument landing system (ILS), or may terminate inside that coverage area (typically at the final approach fix). In the former case, aircraft are vectored to the ILS. In the latter case, vectoring is not typically required once the aircraft is cleared for the RNAV arrival. The RNAV arrival depicted in Fig. 2 is for the same arrival stream and runway as in Fig. 1.

There are two ways to manage the vertical component of an RNAV arrival. In the first, controllers give pilots altitude and speed targets by voice, which pilots then achieve manually or via the autopilot. In the second, altitude and speed constraints at certain waypoints are preprogrammed in the FMS navigation database, and the FMS and autopilot compute and fly a path that satisfies all constraints.

C. Proposed Operational Concept

In previous studies [9–11], controllers were asked to use speed control as the primary means of spacing and to keep aircraft on the RNAV path as long as possible, thereby maximizing the intended benefits. Heading vectors were only to be used when speed control was not sufficient. In these studies, spacing between aircraft at the handoff was assumed the same as for conventional arrivals.

In this paper, a new conceptual framework is proposed in which the role of controllers during RNAV arrivals is divided into four phases: merging and sequencing, spacing, monitoring, and intervention. An intermediate metering point (or simply metering point) separates the descent from cruise and the descent to the runway. Target spacing between consecutive aircraft is given for the metering point such that there is a desired probability that the separation minima can be assured throughout the rest of the RNAV arrival without controller intervention. Before the metering point, controllers are free to vector aircraft as necessary for merging and sequencing, and to establish the target spacing (altitude and speed as well, if so desired). With these initial conditions properly set, aircraft can continue the RNAV arrival without further vectoring. In this phase, controllers monitor the spacing between aircraft, and only intervene if additional spacing is required to prevent separation violations or if a missed approach is necessary. Additional spacing is achieved by changing the speed profile, vectoring the aircraft off the RNAV path and returning it to the path when proper spacing is reestablished, extending the downwind leg, or by sidestepping to an alternate runway.

A strength of the proposed concept of operations is that RNAV arrivals are performed without interruption as long as possible, which is essential to achieving many of the desired benefits. Ideally, RNAV arrivals should be started as far away from the runway as possible: for example, before top of descent. However, the farther the metering point is from the runway, the greater the target spacing must be, as larger buffers must be added to compensate for the larger trajectory variations that build up over longer distances. Thus, the location of the metering point must be tailored to the traffic level. In lighter traffic, it can be moved farther away from the runway. In heavier traffic, it must be moved closer to the runway. This provides great operational flexibility for near-term implementation.

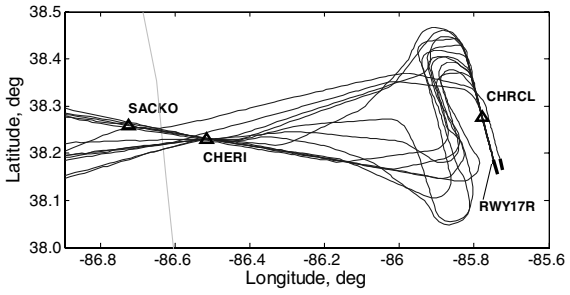

Fig. 1 Sample vectored flight tracks.

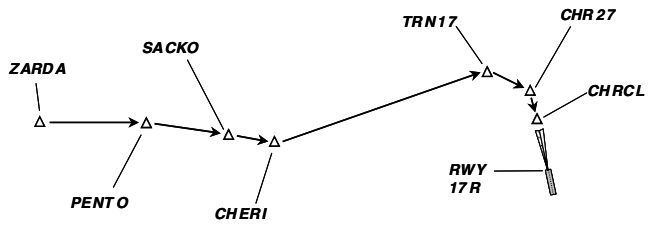

Fig. 2 The lateral flight path of a RNAV procedure.

III. Separation Analysis Methodology

The separation analysis methodology that is presented in this section may be used to analyze the evolution of the spacing between aircraft conducting RNAV arrivals to the same runway, and to determine the target spacing at the metering point. The methodology may also be used to determine the conditions under which the proposed operational concept may be applied.

A. Separation Minima

Under Instrument Flight Rules (IFR), the FAA radar separation minima for aircraft at the same altitude are 3 nautical miles (nm) between aircraft operating within 40 nm (60 nm for single sensor ASR–9 radar with Mode S) of the radar antenna site, and 5 nm between aircraft operating beyond 40 nm (or 60 nm) from the antenna site [12,13]. These minima may be increased or decreased in certain specific situations.

Wake turbulence procedures specify increased separation minima for certain classes of aircraft [12,13]. For the purposes of wake turbulence separation minima, aircraft are classified according to their maximum certificated takeoff weights as heavy, large, and small (with the exception that the Boeing B757 is a large aircraft but is treated specially when it is in a leading position).

In addition to the separation minima, letters of agreement between ATC facilities may define some higher miles-in-trail (MIT) restrictions (such as 10 nm) limited to specified routes and/or sectors/positions during certain periods of the day.

B. Trajectory Variation and Separation

Distance vs time (as depicted in Fig. 3) is the most important relationship when analyzing the separation between consecutive aircraft flying along the same path. In the figure, the horizontal axis represents the along-track distance, and the vertical axis represents

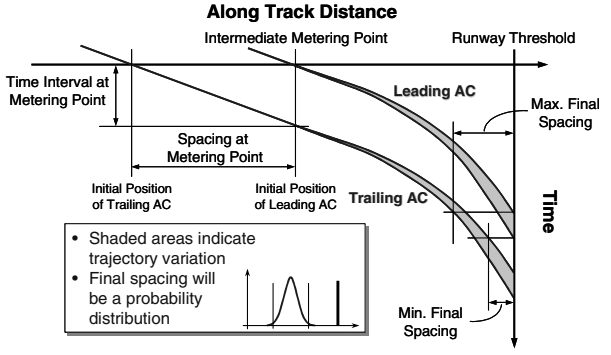

Fig. 3 Trajectory variations and separation.

time. The shaded areas represent the region of uncertainty in the distance–time space where each aircraft could be in the future. For a given spacing at the metering point (measured when the leading aircraft is at the metering point), the final spacing (measured when the leading aircraft is at runway threshold) would be a probability distribution as illustrated in the panel in the figure. Note that the probability density function (PDF) of the final spacing at runway threshold is usually not normal. In this section, all PDFs are shown as similarly shaped bell curves for the sake of simplicity. The minimum value of the final spacing would be given by the slowest leading trajectory and the fastest trailing trajectory, and the maximum value would be given by the fastest leading trajectory and slowest trailing trajectory.

For RNAV arrivals terminating outside the coverage area of ILS, the spacing at the termination point would have similar properties. Thus, without loss of generality, only RNAV arrivals leading to the final approach fix are considered in the rest of this paper.

For a given spacing at the metering point, the minimum value of the probable spacing between any pair of consecutive aircraft (based on a larger number of trajectories) will occur when the leading aircraft is at the runway threshold [14] because of the separation compression due to deceleration, and the variations in aircraft trajectories. Thus, although different separation minima are enforced at different stages of the arrival, the separation minima in effect at the runway threshold are the binding constraints. The target spacing, to be enforced at the metering point, for a given pair of aircraft may therefore be determined by the spacing at the metering point that gives a final spacing distribution whose minimum value is equal to the separation minimum for that pair. However, the target spacing determined in this way is conservative in terms of throughput because one would be protecting against a rare worst-case scenario. Furthermore, the tail of the final spacing distribution might never be known.

On the other hand, the PDF of the final spacing for a given spacing at the metering point may be estimated through analysis of large numbers of aircraft trajectory pairs. Therefore, the target spacing can be determined by adjusting the spacing at the metering point and the resulting estimated distribution of the final spacing at the runway threshold until there is sufficient probability that the final spacing will be greater than or equal to the separation minimum. This process is illustrated in Fig. 4. Note that in this figure, the target spacing is given at the metering point, whereas the separation minimum shown and the final spacing is at the runway threshold. They are overlaid in the same figure to illustrate the relationship. The probability that the procedure can be completed without controller intervention (i.e., the probability of uninterrupted execution) is the integral of the PDF from the separation minimum to infinity, as shown by the shaded area in the figure.

The final separation buffer β_f shown in Fig. 4 is a measure of how much the final spacing will be above the separation minimum, and it is computed by taking the difference between the mean of the final spacing s_f and the separation minimum. This measure can be used as an indicator of efficiency for the selected target spacing. Another measure of efficiency is the average throughput C computed at the metering point in terms of aircraft per hour (1/h) and given by

$$C = 3600/E(T) \tag{1}$$

where $E(T)$ is the mean of interarrival time T in seconds measured at the metering point.

It is worth mentioning that because of the nonlinearity in the distance–time relationship, a different PDF will result in each time the spacing at the metering point is adjusted. That is to say, not only will the PDF of the final spacing shift left or right (see Fig. 4), its standard deviation and the shape will also change. Thus, it is not computationally efficient to determine the target spacing by adjusting the spacing at the metering point and then examining the final spacing. In the next subsection, a method is introduced for determining the PDF of the "feasible spacing" at the metering point that results in a given separation minimum at the runway threshold.

C. Inverse Separation Analysis Problem

Consider a large pool of paired aircraft trajectories. For a specific pair of trajectories, the shaded areas in Fig. 3 would collapse to two curved lines, as shown in Fig. 5. Assume that the leading trajectory and the trailing trajectory in the pair are independent of each other. In this case, the minimum feasible spacing, the minimum spacing at the metering point that assures the separation minimum for the specific pair, can be determined by moving the trailing trajectory in the direction parallel to the time axis until the final spacing is equal to the separation minimum in effect at the runway threshold. In reality, different separation minima would be in effect at different points along the arrival path (see the dashed curve in Fig. 5). Thus, to determine the minimum feasible spacing for a trajectory pair that is already known, separation minima throughout the arrival, not just the final separation minimum, should be protected. It is worth to iterate that, if the actual spacing at the metering point for a specific pair of trajectories is greater than the corresponding minimum feasible spacing, safe separation can be assured for the pair without controller intervention. In other words, if the minimum feasible spacing is smaller than the actual spacing at the metering point, the RNAV procedure can be executed without interruption.

It can be seen from Figs. 3 and 5 that the minimum feasible spacing depends on the separation minima, the location of the metering point, and the characteristics of both the leading and the trailing trajectories. If the leading aircraft is slow and the trailing aircraft is fast, a relatively large minimum feasible spacing would be expected, and vice versa.

For given separation minima, the minimum feasible spacing for a random trajectory pair would be a probability distribution as illustrated in the panel in Fig. 5. This probability distribution may be determined using a large number of minimum feasible spacing values that are obtained when the process already described for a specific pair of trajectories is applied to all available trajectory pairs. By definition, the frequency distribution density of these values normalized by the number of values would, as the number of values gets very large, become the PDF of the minimum feasible spacing. For a selected target spacing, the probability of uninterrupted execution is the probability that the minimum feasible spacing is smaller than the target spacing. This probability can now be computed by integrating the PDF of the minimum feasible spacing from zero to the target spacing (the cumulative probability). The

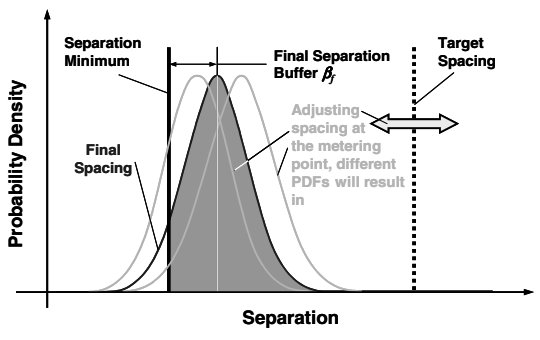

Fig. 4 Adjusting spacing at metering point for final spacing.

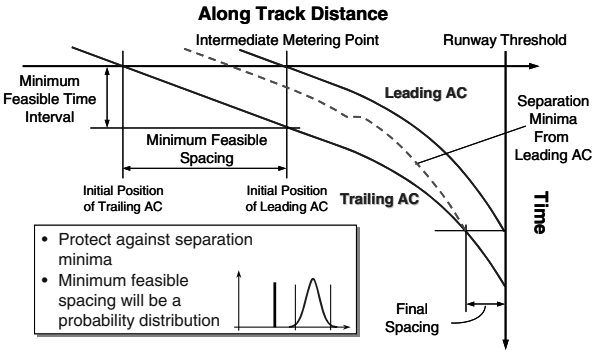

Fig. 5 The inverse separation analysis problem.

probability would be roughly equivalent to the probability obtained using the PDF of final spacing corresponding to the same target spacing (by integrating the PDF from the separation minimum to infinity), but without the need to regenerate the PDF of final spacing for a different target spacing.

The probability is actually the likelihood that, should an aircraft pair arrive at the metering point with spacing exactly equal to the selected target spacing, the procedure can be completed without controller intervention. The probability is thus a conditional probability. With the PDF of the minimum feasible spacing known, a chosen target spacing immediately gives the conditional probability of uninterrupted operation.

D. Conditional Probability Separation Analysis Method

The sequence of aircraft in a consecutive pair is important in determining the target spacing, as aircraft trajectories are functions of the dynamics of the specific aircraft involved, and the applicable separation minima depend on the aircraft weight classes. This is illustrated in Fig. 6 by the PDFs of the minimum feasible spacing for complementary sequences: the first for aircraft type A leading type B; the second for aircraft type B leading type A. Note that the two PDFs in the schematic graph are shown with same shape for the sake of simplicity. In reality, the shape of the PDFs may very well be different. One reason for the difference between the PDFs would be the difference in the weight classes of the aircraft. For example, when a heavy aircraft is leading a large aircraft, the separation minimum is greater than in the complementary case. Thus, the minimum feasible spacing would probably also be larger. Another reason would be the difference in the performance characteristics of the aircraft. For example, if one aircraft descends at a steeper angle than the other, the steeper aircraft has a higher ground speed for longer even if the two aircraft descend at the same indicated airspeed (IAS). Of course, the difference between the PDFs could also result from a combination of both reasons. The sequences with aircraft of the same type, aircraft type A leading type A and type B leading type B, are not shown in Fig. 6, also for the sake of simplicity.

1. *Sequence-Independent Target Spacing*

Given the probability density p_i of the minimum feasible spacing for aircraft sequence i, and a target spacing S_I, the conditional probability P_{Ri} of uninterrupted execution is

$$P_{Ri} \equiv P(\text{uninterrupted}|s_T = S_I) = P(s \le S_I) = \int_0^{S_I} p_i \, \mathrm{d}s \quad (2)$$

where s denotes the minimum feasible spacing, s_T denotes spacing at the metering point, and subscripts R denotes that the probability is conditional. The integral is shown by the shaded areas under the two PDFs in Fig. 6. The conditional probability of uninterrupted execution is the probability that there will be no separation violations in an uninterrupted RNAV arrival stream if (on the condition that) the spacing at the metering point is exactly equal to the selected target spacing S_I.

If the aircraft sequences have different PDFs of the minimum feasible spacing, as shown in Fig. 6, each aircraft sequence will have a different conditional probability for the same target spacing. The difference in conditional probability is illustrated in Fig. 6 by the difference in the areas of the shaded regions under the PDFs. Thus, if a single target spacing is desired, to be consistent with the current practice of having a single MIT restriction for the entire traffic stream at the handoff or metering point, it could be determined by finding the minimum S_I such that every single P_{Ri}, or the average of P_{Ri}, is greater than or equal to the desired value.

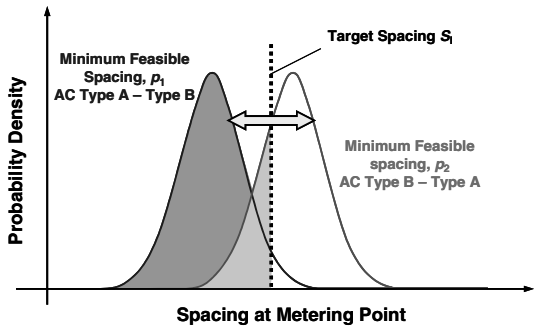

Fig. 6 Conditional probability method.

2. *Sequence-Specific Target Spacings*

To have the same conditional probability for all sequences, each aircraft sequence must have a different target spacing. Although such a scheme is more complex, there is a strong motivation for it. If a single target spacing is used, it will be too conservative for some aircraft sequences. By using sequence-specific target spacings, throughput may be increased.

The conditional probability separation analysis method using sequence-specific target spacings is illustrated in Fig. 7. The light gray dotted vertical line in the middle denotes the sequence-independent target spacing for both aircraft sequences. This target spacing would give a certain average conditional probability. However, as mentioned earlier, for each of the aircraft sequences, the sequence-independent target spacing would give a different conditional probability. The dotted vertical line on the left corresponds to the target spacing for aircraft type A leading type B with a conditional probability that is equal to the average level given by the sequence-independent target spacing. The dotted vertical line on the right is the corresponding target spacing for aircraft type B leading type A. Sequence-specific target spacings would give the same conditional probability for different aircraft sequences, as illustrated by the areas of shaded regions under PDFs.

For relatively high probabilities, the use of sequence-specific target spacings would give a lower average target spacing. This is further illustrated in Fig. 8. In this figure, cumulative probabilities for the two aircraft sequences are shown as individual functions, and as an average. If sequence-specific target spacings with the same conditional probability are used, as indicated in the figure, a smaller target spacing would be needed for aircraft type A leading type B, and a larger target spacing would be needed for aircraft type B leading type A. For the conditional probability shown, the decrease

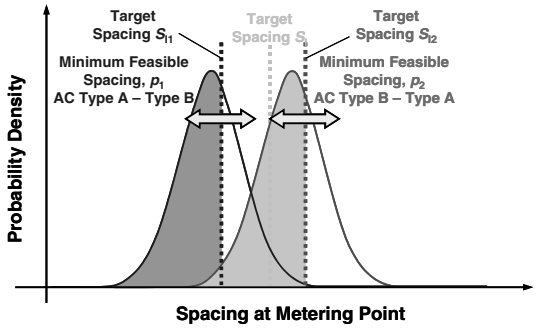

Fig. 7 Sequence-specific conditional probability method.

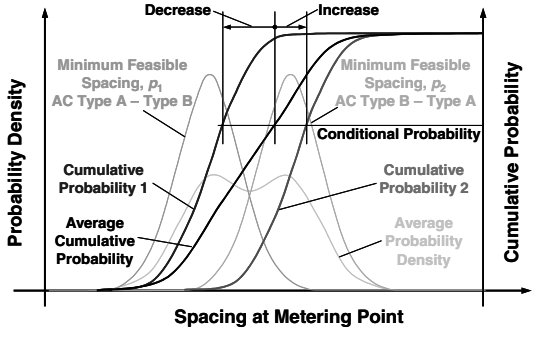

Fig. 8 Sequence-specific separation capacity savings.

in the target spacing for aircraft type A leading type B is greater than the increase for aircraft type B leading type A. Thus, the average target spacing will be lower, and throughput will be increased.

As the conditional probability increases, the difference will be even greater, giving an even smaller average target spacing thus greater throughput. In other words, this would result in a smaller final separation buffer. Given the target spacing S_{Ii} for aircraft sequence i, Eq. (2) now becomes

$$P_{Ri} \equiv P(\text{uninterrupted}|s_T = S_{Ii}) = P(s \le S_{Ii}) = \int_0^{S_{Ii}} p_i \, \mathrm{d}s \quad (3)$$

E. Total Probability Separation Analysis Method

A key assumption in the conditional probability separation analysis method is that the spacing at the metering point is exactly equal to the target spacing. The reality is that neither controllers nor automation are this precise. Thus, there will always be some variability in the spacing at the metering point, and this variability must be accounted for if the total probability of uninterrupted execution is to be determined.

1. *Characteristics of Spacing in Arrival Stream*

To this end, it is necessary to characterize the actual spacing in the arrival stream at the metering point. A hypothetical PDF of the spacing at the metering point subject to a given target spacing (or MIT restriction) is illustrated by the solid black curve in Fig. 9.

Should a higher target spacing be used, as a result of controllers' effort to achieve that target, the PDF of the spacing at the metering point will be shifted towards higher values, that is, rightwards. This is illustrated by the gray curve in Fig. 9. The traffic stream with the increased target spacing is referred to as the adjusted traffic. The shapes of the PDFs are not symmetrical because controllers normally only need to make adjustments if the spacing could fall below the target spacing. Notice that in the figure, the tails of the PDFs extend to the left of target spacing. This is to illustrate that, on rare occasions, the spacing may actually be less than the target spacing. However, this is typically not an issue as target spacings (as will be shown later) are much higher than the separation minima in effect at the metering point.

The mean spacing at the metering point for the unadjusted traffic stream, an indicator of arrival traffic volume, is given by

$$E(s_T) = \int_0^{\infty} p_T s \, \mathrm{d}s \quad (4)$$

The mean spacing for the adjusted traffic stream is simply

$$E(s_{Ta}) = \int_0^{\infty} p_{Ta} s \, \mathrm{d}s \quad (5)$$

In practice, the lower integration limit in Eqs. (4) and (5) would be the separation minimum in effect at the metering point because the integral from zero to the separation minimum should be zero. However, zero is used as the lower integration limit throughout this paper for the sake of simplicity.

When the arrival rate is below the runway acceptance rate, the mean unadjusted traffic spacing will be much higher than the separation minimum that is in effect at the metering point. As the arrival rate increases, the PDF of the spacing at the metering point will become narrower, and the mean will be closer to the separation minimum.

A natural metering point at which the requisite data can be collected is the boundary between the CENTER and the TRACON, because this is the point where the handoff of aircraft occurs. The distribution of the unadjusted traffic spacing can be obtained from radar data, as can the distribution of adjusted traffic spacing. The distribution of spacing can also be obtained through controller-in-the-loop simulations.

2. *Total Probability for Unadjusted Traffic*

Once the PDF p_T of the unadjusted traffic spacing, such as that shown in Fig. 9 is known, a total probability can be computed. The probability [referring to Fig. 10 and based on Eq. (2)] that aircraft sequence i would be contained in the small slice of traffic at spacing s, and could execute the procedure without interruption is

$$\mathrm{d}P_{T,i,s} = p_T \, \mathrm{d}s \int_0^s p_i \, \mathrm{d}x \quad (6)$$

On the left-hand side of Eq. (6), subscript T denotes that the probability is from the PDF of unadjusted traffic spacing. The integral on the right-hand side of Eq. (6) is actually the cumulative probability of the minimum feasible spacing. The total probability $P_{T,i}$ of uninterrupted execution for aircraft sequence i under the unadjusted traffic can be obtained using

$$P_{T,i} = \int_0^{\infty} \left(\int_0^s p_i \, \mathrm{d}x \right) p_T \, \mathrm{d}s \quad (7)$$

For the probability P_i that aircraft sequence i is in the arrival traffic stream, the overall total probability P_T of uninterrupted execution under the unadjusted traffic is a weighted average of total probabilities for all aircraft sequences, that is,

$$P_T = \sum_i P_i P_{T,i} = \sum_i P_i \int_0^{\infty} \left(\int_0^s p_i \, \mathrm{d}x \right) p_T \, \mathrm{d}s \quad (8)$$

The probability given by Eq. (8) now depends on the actual traffic condition, that is, traffic mix and the distribution of unadjusted traffic spacing. For example, if there is only a small percentage of the sequence where a heavy is leading a small (a sequence with large minimum feasible spacing, and a PDF farther to the right than for other sequences), that sequence will not contribute much to the overall total probability. Note that once the PDF of unadjusted traffic spacing and ground speed are known, the average arrival rate can be estimated. However, the PDF of unadjusted traffic spacing is not unique for a given average arrival rate even if ground speed is fixed. Equations (7) and (8) not only account for the arrival rate, they also account for the randomness in the arrival stream. For the same average arrival rate, higher randomness will give a flatter p_T, yielding lower total probability.

The overall total probability gives an estimated percentage of flights in the arrival stream that could execute the procedure without

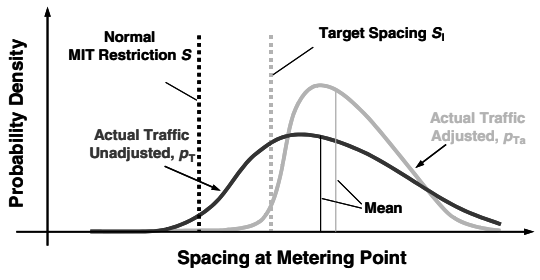

Fig. 9 Spacing distribution in incoming traffic stream.

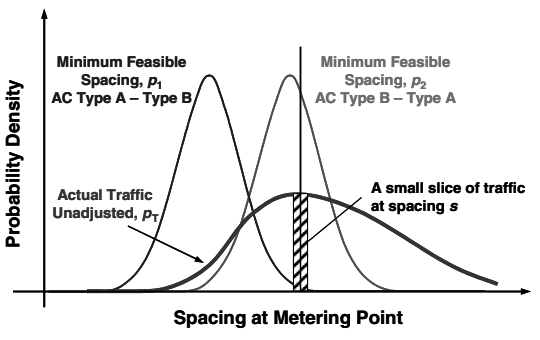

Fig. 10 Probability under normal traffic flow.

any controller intervention. This total probability is an indicator of how well the procedure fits into the actual traffic flow, that is, without the need to impose a higher target spacing at the metering point. Under lighter traffic conditions, the PDF p_T will shift to the right, yielding higher values of P_T. This means the procedure could be executed without controller intervention at a higher probability. Under heavier traffic conditions, the PDF p_T will shift to the left, yielding lower values of P_T. This means the procedure could be executed without controller intervention only at a lower probability.

3. Sequence-Independent Target Spacing

When a higher target spacing is used, the PDF of the spacing in (adjusted) traffic would be similar to the thick gray curve in Fig. 11. Following the same derivation as in the preceding subsubsection, the total probability for aircraft sequence i under the adjusted traffic $p_{T,a}$ is given by

$$P_{Ta,i} = \int_0^\infty \left(\int_0^s p_i \, \mathrm{d}x \right) p_{Ta} \, \mathrm{d}s \tag{9}$$

The overall total probability P_{Ta} under the adjusted traffic is

$$P_{Ta} = \sum_i P_i P_{Ta,i} = \sum_i P_i \int_0^\infty \left(\int_0^s p_i \, \mathrm{d}x \right) p_{Ta} \, \mathrm{d}s \tag{10}$$

As can be seen in Fig. 11, the PDF of the adjusted traffic spacing is to the right of the PDF for the unadjusted traffic, resulting in a higher total probability. Thus, the goal of the total probability method is to find the minimum target spacing S_I such that the resulting probability density p_{Ta} would assure an overall total probability P_{Ta} that is greater than or equal to the desired value.

When traffic is not heavy, the mean traffic spacing would increase at a much slower rate than the increase in the target spacing. In other words, the arrival rate would decrease at a much slower rate than the rate at which the target spacing is increased. This is because, when traffic is not heavy, the increase in the target spacing would mostly reduce spacing randomness in the arrival stream rather than increase the mean traffic spacing. However, when traffic is heavy, the increase in the target spacing would at some point cause the arrival rate to decrease. In this case, a tradeoff must be made between RNAV procedure benefits and throughput. This will be discussed in more detail later.

4. Sequence-Specific Target Spacings

The total probability separation analysis method using sequence-specific target spacings is illustrated in Fig. 12. By using sequence-specific target spacings, the spacing at the metering point for each aircraft sequence will be adjusted by the controller based on the target spacing for that specific aircraft sequence, as shown by the PDFs (thick gray curves annotated by actual traffic, adjusted p_{Ta1} and p_{Ta2}) for adjusted traffic spacing in Fig. 12. Note that both the means and shapes of the PDFs for the adjusted traffic spacing would be different for different target spacings. However, these PDFs would likely only depend on the PDFs of the unadjusted traffic spacing and the target spacing used, but not the aircraft sequence, because controllers

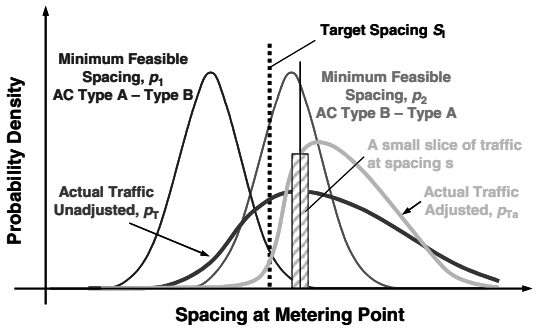

Fig. 11 Probability under adjusted traffic flow.

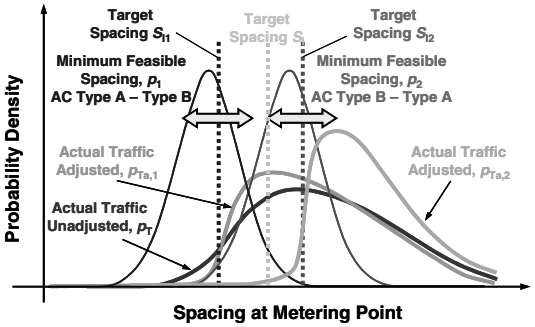

Fig. 12 Sequence-specific total probability method.

probably would not treat each aircraft differently. Based on this assumption, a generic model of PDFs for the adjusted traffic spacing may be developed that would be applicable to different aircraft types.

Now the PDF of the adjusted traffic spacing for aircraft sequence i becomes $p_{Ta,i}$. Referring to Figs. 10 and 11, the probability that aircraft sequence i would be contained in the small slice of traffic at spacing s and could execute the procedure without controller intervention is

$$\mathrm{d}P_{Ta,i,s} = p_{Ta,i} \, \mathrm{d}s \int_0^s p_i \, \mathrm{d}x \tag{11}$$

In Eq. (11), subscripts Ta, i denote that the probability is from the PDF of adjusted traffic spacing under the target spacing for aircraft sequence i. Similarly, the total probability that all aircraft pairs of sequence i in the traffic stream could execute the procedure without further controller intervention is

$$P_{Ta,i} = \int \mathrm{d}P_{Ta,i,s} = \int_0^\infty \left(\int_0^s p_i \, \mathrm{d}x \right) p_{Ta,i} \, \mathrm{d}s \tag{12}$$

The overall total probability for all aircraft sequences then becomes

$$P_{Ta} = \sum_i P_i P_{Ta,i} = \sum_i P_i \int_0^\infty \left(\int_0^s p_i \, \mathrm{d}x \right) p_{Ta,i} \, \mathrm{d}s \tag{13}$$

Note that the sum of probability P_i for all aircraft sequences in the arrival traffic stream is equal to one. Thus, by selecting S_{Ii} such that $P_{Ta,i}$ is equal to the desired value, the resulting overall total probability would also be equal to the same desired value. This observation offers a simple way to determine sequence-specific target spacings using the total probability method: that is, by determining each target spacing independently.

F. Tradeoff Analysis

In both the conditional probability and the total probability separation analysis methods, the individual sequence-specific target spacing for each of the aircraft sequences can be determined independently with the same probability. Target spacing determined this way treat each of the aircraft sequences equally even though their contribution to throughput or overall probability may very well be different. Under some situations, it may be better to assign different probabilities for different aircraft sequences.

For instance, if a specific aircraft sequence requires a much larger minimum feasible spacing than other sequences, and the sequence is rare in the arrival stream, it might not be prudent to simply use a large target spacing for this aircraft sequence. Rather, a moderate target spacing could be used for this specific aircraft sequence if there is some tolerance for aircraft in this sequence being vectored during the descent when deemed necessary. On the other hand, target spacing slightly higher than that specified by the average probability could be used for aircraft sequences that require smaller minimum feasible spacing to allow more aircraft of those sequences to perform RNAV arrivals without interruptions. The benefits of this strategy are twofold. First, by using sequence-specific target spacings that are

determined with different probability, the throughput may be increased even for the same overall probability, or higher overall probability may be achieved for the same throughput. Second, by eliminating the use of very large target spacing that might be nominally required by some rare aircraft sequences, excessive delay to other aircraft behind those aircraft sequences may be avoided.

Two optimization problems can be formulated for the sequence-specific target spacings using the total probability method. In the first optimization problem, traffic delay is minimized for the given overall total probability. Mean adjusted traffic spacing at the metering point is used as the indicator of traffic delay caused by spacing adjustment. A more direct indicator of traffic delay is the average interarrival time at the metering point. The connection between the two is ground speed. The mean adjusted traffic spacing subjected to a single target spacing is given in Eq. (5). The objective in this problem is to choose sequence-specific target spacing S_{Ii} to minimize the mean adjusted traffic spacing

$$E(s_{Ta}) = \sum_i P_i \int_0^\infty p_{Ta,i} s \, \mathrm{d}s \tag{14}$$

subject to the constraint

$$P_{Ta} = \sum_i P_i \int_0^\infty \left(\int_0^s p_i \, \mathrm{d}x \right) p_{Ta,i} \, \mathrm{d}s \geq P_{Ta}|_{\text{given}} \tag{15}$$

In the second optimization problem, the objective is to choose S_{Ii} to maximize the overall total probability as given in Eq. (13), for given traffic conditions, that is, the mean adjusted traffic spacing shall not exceed the mean unadjusted traffic spacing

$$E(s_{Ta}) \leq E(s_T) \tag{16}$$

The constraint given in Eq. (16) implies that only the randomness in spacing is reduced when target spacings are imposed to improve the total probability. Because average spacing is not increased, no additional delay is introduced. The mean unadjusted traffic spacing is given in Eq. (4). For the sake of clarity, the second problem is rewritten as choosing S_{Ii} to maximize

$$P_{Ta} = \sum_i P_i \int_0^\infty \left(\int_0^s p_i \, \mathrm{d}x \right) p_{Ta,i} \, \mathrm{d}s \tag{17}$$

subject to the constraint

$$\sum_i P_i \int_0^\infty p_{Ta,i} s \, \mathrm{d}s \leq \int_0^\infty p_T s \, \mathrm{d}s \tag{18}$$

In the first optimization problem, defined by Eqs. (14) and (15), additional delay may have to be introduced as the given total probability increases. In the second optimization problem, defined by Eqs. (17) and (18), the total probability may be limited to a certain level when the traffic is heavy. The optimal solution from the second problem gives the highest overall total probability that could be achieved without introducing additional delay. The solution from the first problem, on the other hand, gives the maximum throughput (connected to minimum spacing via ground speed) that could be achieved for the given desired overall total probability.

Although detailed analyses of RNAV procedure benefits and delay penalties are out of the scope of this paper, the formulations of the two optimization problems provide bases for more rigorous tradeoff analysis in the future. This tradeoff may be illustrated as follows: To maintain throughput, the average spacing at the metering point needs to be kept as low as possible so that additional delay is not imposed to upper stream traffic. This suggests the selection of a target spacing that is as close as possible to the separation minima or MIT restrictions currently being used, or the use of a relatively low probability of uninterrupted execution. However, the benefits of RNAV arrivals are best achieved when there are no interruptions. This suggests the selection of larger target spacing, or a relatively high probability. The optimum solution is a tradeoff between the solutions of the two optimization problems. It is important to note that this tradeoff is only possible because of the controller's ability to predict separation violations and intervene when necessary. Additionally, the location of the metering point may be moved towards or away from the runway to search for a better design if the optimal solution at the current metering point is not satisfactory.

In current practice, MIT restrictions at the metering point or handoff point are given as a single number for the entire traffic stream at any given time. Using sequence-specific target spacings will increase the number of variables for the controller to work with. For example, with two aircraft types A and B, four aircraft sequences exist. As the number of aircraft types increases, the number of aircraft sequences increases geometrically. To be practical, the number of sequence-specific target spacings must be limited to a manageable level. Moreover, MIT restrictions are discretized [15], often in increments of 5 nm. However, the optimal target spacing are continuous variables and thus may fall between the discrete MIT restriction values currently in use. These target spacing must also be discretized to some degree for easy handling.

As an option, aircraft sequences with similar minimum feasible spacing distributions could be consolidated to simplify the scenario. The optimization method could then be modified to accommodate the discretization requirement. In any case, for optimal performance, the discretization step size will have to be reduced from the commonly used 5 nm.

IV. Modeling Trajectory Variations

The separation analysis methodology introduced in the preceding section requires analyses of aircraft trajectory variations. Unlike conventional arrivals, large volumes of historical data from uninterrupted RNAV arrivals are often not readily available. Thus, a computer simulation has been developed to generate the aircraft trajectories. A brief description of the tool is given in this section to facilitate further discussion. Readers are referred to [16,17] for a complete description.

A. Components of the Monte Carlo Simulation Tool

Under the proposed conceptual framework, trajectory variations occur in two stages. First, the flight path built by the onboard FMS may vary from flight to flight even for the same procedure. Second, uncertainties encountered during the execution of the procedure cause deviations from the FMS flight path. Contributing factors to aircraft trajectory variations were identified as 1) aircraft type: differences in aircraft design and dynamics, 2) RNAV descent path logic: difference in aircraft equipage and design, 3) aircraft weight: variation due to demand and operation conditions, 4) pilot technique: variations among pilots and pilot response randomness, and 5) weather conditions: predominantly variation in winds.

To ensure the simulation accuracy, careful considerations had to be taken in modeling each of the components. The central piece of the Monte Carlo simulation tool is a fast-time aircraft simulator. The dynamics of the aircraft is determined using a point-mass model based on non-steady-state equations of motion and is thus more accurate in simulating wind effects than an ordinary point-mass model based on steady-state equations of motion. Aerodynamic coefficients are modeled as functions of angle of attack, flap and gear settings, speed brake position, and Mach number. The model for each aircraft type was developed based on aerodynamic data and installed engine performance data provided by aircraft manufacturers. The autopilot, the autothrottle, and the FMS lateral navigation (LNAV) and vertical navigation (VNAV) capabilities are also modeled. Although the FMS computed lateral path can be more precise by using Required Navigation Performance (RNP) procedures [18] (for RNP capable system), the FMS VNAV logic is more complex. Given the same procedure design (vertically defined as altitude and speed constraints at certain waypoints), FMS computed vertical path will vary with aircraft types and configurations. These differences are captured by the FMS module in the aircraft simulator.

Because aircraft weight and performance parameters are used by the FMS to compute the VNAV path, a different aircraft weight will result in a different VNAV path. Furthermore, the dynamics of the

aircraft will also be different. Historical data collected from airline operations were used to model the distribution of the aircraft landing weight for each aircraft type.

A pilot agent is included in the aircraft simulator to control the extension of flaps, landing gear, and speed brakes. For each aircraft type, the flap schedule in the aircraft operation manuals, such as the UPS B757/767 manual [19], may be used, or the flap schedule can be tailored to the given RNAV procedure. The pilot response delay model obtained from a previous human-in-the-loop B747-400 simulation study [20] is included in the pilot agent.

Winds are the most significant single factor affecting aircraft trajectories. All else being equal, the FMS flight path is a function of wind forecast and the current winds as measured by the onboard sensors at the time the path is computed [17]. Further, wind uncertainties during the descent affect the aircraft's ability to follow the computed flight path.

Winds are modeled using nominal profiles that reflect long-term statistical expectations, and short-term variations that reflect wind changes between consecutive flights. A unique mode decomposition and autoregressive technique was developed to model wind variations between flights [17]. Specific wind models are developed using Aircraft Communications Addressing and Reporting System (ACARS) automated weather reports by commercial aircraft as archived by the National Oceanic & Atmospheric Administration (NOAA) [21,22].

B. Tool for the Analysis of Separation and Throughput

The random pilot response model, the random aircraft weight model, and the random wind model have been combined with the fast-time aircraft simulator to form an integrated Monte Carlo simulation tool. This Monte Carlo tool is used to simulate a given RNAV arrival hundreds of times with different aircraft types and configurations under different wind conditions. The simulated trajectories are then used for separation analysis. The Monte Carlo tool and the separation analysis methodology form a Tool for the Analysis of Separation and Throughput (TASAT) as illustrated in Fig. 13.

During each simulation run, a unique aircraft landing weight is generated for the given aircraft type by the random model. The wind profile is also different for each simulation run. Pilot response time is randomly generated for each of the control actions. It is assumed that there is no direct interaction between consecutive flights performing the same procedure. Thus, when multiple aircraft types are involved in a procedure, each aircraft is simulated separately.

Table 1 RNAV procedure vertical constraints

Waypoint	D, nm	H, ft	IAS, kt
TRN17	−11.6	Above 4000	——
CHR25	−8.1	3000	180
CHRCL	−5.6	2350	170
Runway	0	——	——

The application of the wind model needs special attention. To make best use of the interflight wind variation model, flights are identified as leading flights or trailing flights. For each aircraft type, an ensemble of flights is simulated with a fixed nominal wind profile while retaining the variations in other factors such as pilot response and weight. Another ensemble of flights is simulated with the nominal wind profile plus the random interflight wind variation in addition to other random factors. A simulated trajectory from the leading ensemble and a simulated trajectory from the trailing ensemble are selected to form a random flight pair. Enumerating flights from each ensemble, a large number of flight pairs is constructed. The separation analysis methodology is then applied to those flight pairs accordingly.

V. Simulation Results

A simulation study was conducted to illustrate the application of the separation analysis methodology and TASAT, and to determine the impact of operational conditions and procedure design parameters on throughput. The results of that study are presented in this section.

A. Simulation Setup

The arrival procedure used in the simulation was based on an experimental RNAV arrival procedure developed for Louisville International Airport-Standiford Field (KSDF) runway 17R. The lateral profile of this procedure is shown in Fig. 2. The altitude (H) and IAS constraints that define the vertical profile of this procedure are listed in Table 1. The descent speed was IAS 350 kt from cruise to 10,000 ft, and IAS 240 kt from 10,000 ft to the point where the aircraft began decelerating to satisfy the first speed constraint. Two aircraft types, B757-200 (B757) and B767-300 (B767), were

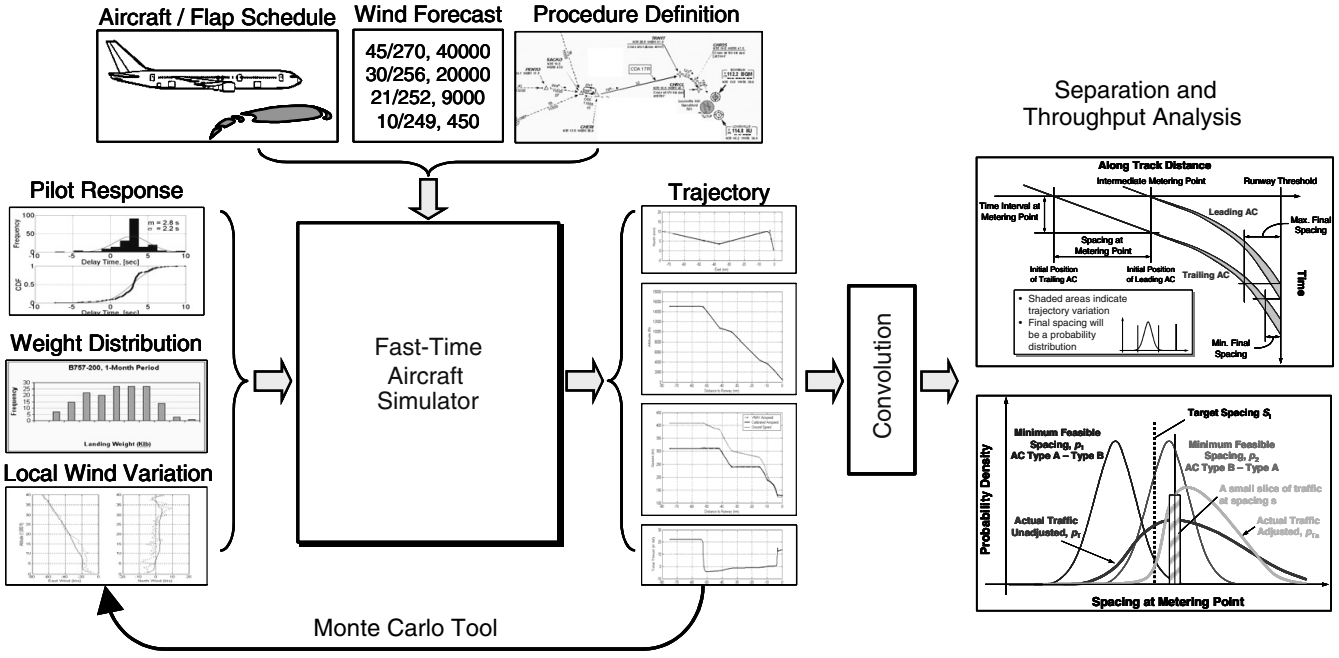

Fig. 13 Tool for the Analysis of Separation and Throughput.

Table 2 Landing weight parameters, lb

	B757-200	B767-300
Mean	167,539	262,205
Standard deviation	11,000	18,000
Minimum	146,617	229,271
Maximum	194,534	298,183

simulated with random landing weights as defined in Table 2. Nominal wind profiles and interflight wind variations were modeled using ACARS data reported between 22:00–3:00 hrs local standard time each day during a period of six months from 10 February to 12 August 2004. For a given scenario, each aircraft type was simulated 200 times in the leading position and 200 times in the trailing position. For the two aircraft types, a total of 800 trajectories were simulated in each scenario. Unless otherwise noted, the mean wind profile was used.

B. Minimum Feasible Spacing and Target Spacing

The PDFs of the minimum feasible spacing at SACKO, which is a waypoint at −53.4 nm track distance or about 10 nm away from the TRACON boundary, were obtained from simulated trajectories. The results are shown in Fig. 14. Each is based on 20,000 simulated trajectory pairs. Among the four possible aircraft sequences, the sequence of B767 leading B757 has the largest values of minimum feasible spacing. This is partially because this sequence has the largest required final separation among the four, that is, 5 nm, whereas the other three required 4 nm. Another factor is that the B757 aircraft, which was in the trailing position, had larger trajectory variations. This latter factor can also be seen by comparing the sequence of B757 leading B757 with the sequence of B767 leading B767.

The PDFs of the final spacing at the runway threshold are shown in Fig. 15 for a target spacing of 15 nm at SACKO. The two vertical lines indicate the separation minima at the runway threshold: the one on the right is for B767 leading B757, the one on the left is for the others.

C. Application of Conditional Probability Method

For a sequence-independent target spacing of 15 nm, the conditional probability for the four aircraft sequences can be computed using either the PDFs of the minimum feasible spacing shown in Fig. 14, or the PDFs of the final spacing shown in Fig. 15. The results are listed in Table 3 as the group of data in the middle. Again, it is important to note that for a different target spacing, the PDFs need to be regenerated for the final spacing whereas the PDFs for the minimum feasible spacing can be reused for any target spacing values. The sequence-specific target spacings are also listed in the table (the right-most group). They were determined for a conditional probability equal to the average of conditional probability for the sequence-independent target spacing of 15 nm. The average of the sequence-specific target spacings was 14.57 nm, 0.43 nm lower than the sequence-independent target spacing. This 0.43 nm reduction in average target spacing was the benefit of using sequence-specific target spacings. Notice that the averages in Table 3 were not weighted. Thus, the average is only applicable to scenarios in which there are 50% of each aircraft type.

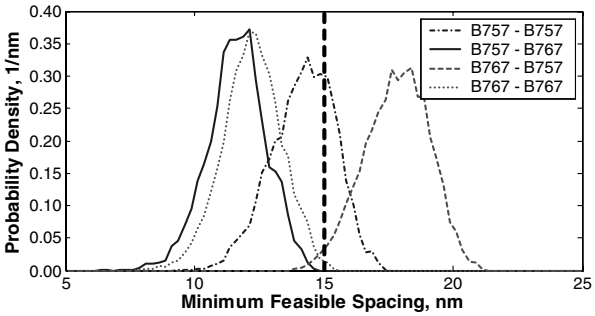

Fig. 14 Minimum feasible spacing at SACKO.

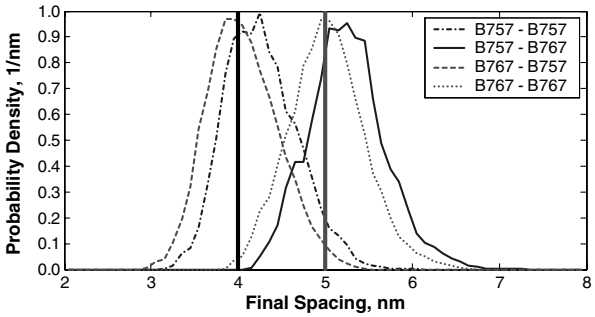

Fig. 15 Final spacing given 15 nm at SACKO.

Other items listed in Table 3 are throughput C and final separation buffer β_f for each aircraft sequence i. The average throughput values are not averages of the individual aircraft sequences. They were directly computed from mean time intervals at SACKO. The throughput values listed in Table 3 have only theoretical meaning because in real world situations the actual spacing would not be exactly equal to the target spacing. The ideal case listed in the table implies that trajectory variations were predicted precisely as they would happen and that the spacing at the metering fix for each consecutive aircraft pair was set exactly to the corresponding minimum feasible spacing. This means there would be no capacity loss in accommodating the uninterrupted RNAV operations, and that the final separation buffer would be equal to zero. Thus, throughputs for the ideal case indicate system capacity for the given aircraft mix. The average throughput was 31.88 aircraft per hour for the ideal case. It is seen that for the same average conditional probability, by using sequence-specific target spacings, the final separation buffer was reduced and more evenly shared by all aircraft sequences. The average traffic throughput was increased from 29.62 to 30.60.

To further illustrate the relationship between the sequence-independent target spacing and the corresponding sequence-specific target spacings, conditional probabilities were computed for a series of sequence-independent target spacing values. For each of the conditional probabilities, sequence-specific target spacings and their average were obtained. This relationship is shown in Fig. 16. It is seen that, at lower probability, that is, below 63%, sequence-specific target spacings actually reduce efficiency. As the probability became greater than 63%, sequence-specific target spacings start to improve efficiency; the higher the probability, the higher the benefits sequence-specific target spacings provide. The reason behind this is graphically illustrated in Fig. 8, and explained earlier.

Table 3 Target spacing, probability, and traffic throughput

Aircraft type/sequence	Ideal case		$S_I = 15$ nm			$P_{Ri} = 68.2\%$		
	C_i	$E(S_i)$	P_{Ri}	C_i	β_{fi}	S_{Ii}	C_i	β_{fi}
B757-B757	32.02	14.21 nm	71.8%	30.40	0.27 nm	14.88 nm	30.63	0.23 nm
B757-B767	36.89	11.64 nm	100.0%	28.88	1.25 nm	12.17 nm	35.32	0.20 nm
B767-B757	25.82	17.82 nm	1.5%	30.40	−0.94 nm	18.47 nm	24.94	0.24 nm
B767-B767	35.18	12.22 nm	99.6%	28.88	1.02 nm	12.76 nm	33.73	0.20 nm
Average	31.88	13.97 nm	68.2%	29.62	0.40 nm	14.57 nm	30.60	0.22 nm

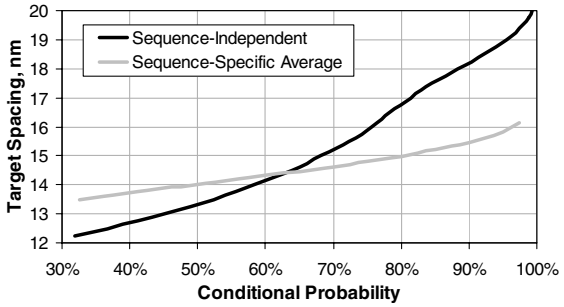

Fig. 16 Target spacing vs probability.

D. Application of Total Probability Method

The total probability separation analysis method requires the distribution of traffic spacings at the metering point. To this end, the spacings at SACKO were extracted from Automated Radar Terminal System (ARTS) data via the UPS ground management system. Flights arriving between 22:00–3:00 hrs local standard time on 28 days between 14 September and 1 December 2004 were examined. On 18 of these 28 days, a 10 nm MIT restriction was in effect; on the remaining 10 days, all in September, a 15 nm MIT restriction was in effect. In total, 131 flight pairs were selected from the arrival stream under 10 nm MIT, and 69 flight pairs were selected from the arrival stream under 15 nm MIT. The estimated PDFs of spacing in the arrival stream are shown as bar charts in Fig. 17. Traffic under 10 nm MIT and 15 nm MIT are denoted as unadjusted traffic and adjusted traffic, respectively. It is normal that at times the MIT restrictions might not be satisfied, as shown by the bars on the left of 10 nm and 15 nm for unadjusted traffic and adjusted traffic, respectively. However, there were no observations of spacing below the separation minimum of 5 nm. Estimated parameters of the spacing in the arrival stream such as mean $E(s)$ and standard deviation σ_s are listed in Table 4. It is seen that although the average traffic spacing was increased by using a larger target spacing, the standard deviation was decreased: indicating a reduction in randomness. It is also seen that as the target spacing increases, the average traffic spacing increases by a smaller amount than the corresponding increase in the target spacing.

An Erlang probability density function [23] was fit to model the spacing data. The Erlang PDF is given by

$$p(s) = \begin{cases} \frac{\lambda^k s^{k-1} e^{-\lambda s}}{(k-1)!} & k = 1, 2, \ldots; s \geq 0 \\ 0 & \text{otherwise} \end{cases} \tag{19}$$

where s is the spacing in arrival stream; and k is referred to as the order of the Erlang PDF, λ is another parameter. For any set of given parameters, the mean and variance are $E(s) = k/\lambda$ and $\sigma^2 = k/\lambda^2$. Given estimated mean and variance, parameters of the Erlang model can be estimated as

$$\begin{cases} k' = \text{round}[E^2(s)/\sigma_s^2] \\ \lambda' = k'/E(s) \end{cases} \tag{20}$$

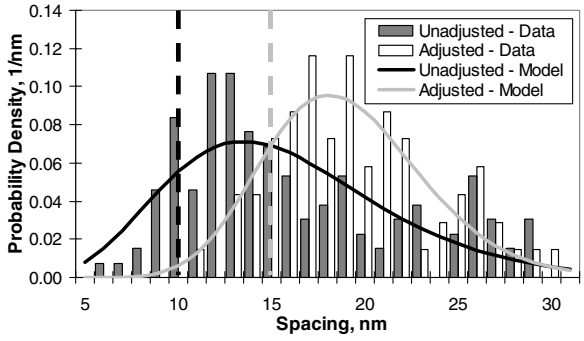

Fig. 17 Traffic spacing at SACKO.

Table 4 Spacing parameters in arrival traffic

Traffic condition	Traffic data		Model	
	$E(s)$, nm	σ_s, nm	k'	λ', 1/nm
Unadjusted	15.79	5.88	7	1.050
Adjusted	19.05	4.28	20	0.443

Table 5 Total probability assuming 50-50 traffic mix of B757 and B767

Sequence	P_T	P_{Ta}
B757-B757	55.6%	87.5%
B757-B767	74.2%	97.1%
B767-B757	33.6%	59.7%
B767-B767	70.3%	95.7%
Overall	58.7%	85.0%

The Erlang approximations to the PDFs of traffic spacing are shown as the solid black curve and the light gray curve in Fig. 17 for 10 nm MIT and 15 nm MIT, respectively. The estimated model parameters are listed in Table 4. It is seen from Fig. 17 that the models fit the data well. With sufficient radar data or simulation data, a generic model for a specific metering point may be developed as a function of the mean of the unadjusted traffic spacing, the standard deviation of the unadjusted traffic spacing, and the target spacing.

With the distributions of the spacing in the arrival stream known, the total probability for the unadjusted traffic and the adjusted traffic can be computed using Eqs. (8) and (10), respectively. The results listed in Table 5 are for a 50-50 traffic mix of B757 and B767 that is randomly sequenced such that there is 25% of each of the four aircraft sequences.

Comparing Table 5 with Table 3 and Fig. 16, it is seen that the total probability values are higher than the conditional probability values for the same target spacing. For a target spacing of 10 nm, the average (as if weighted by 50-50 traffic mix) of the conditional probability was less than 30%, whereas the total probability is 58.7%. For a target spacing of 15 nm, the average of the conditional probability was 68.2%, whereas the total probability is 85.0%.

As these results illustrate, the total probability method provides a more complete view of the relationship between the target spacing and the probability of uninterrupted execution in a real world environment, although extra effort is needed to obtain the distribution of the traffic spacing. It is also important to note that, should the same probability be desired, the total probability method would yield a smaller target spacing.

E. Contributions of Winds

Simulations were conducted with different nominal wind profiles: the mean wind profile, the zero wind profile, and a hypothetical head wind profile. The mean wind profile for KSDF would be experienced as a tail wind during most of the arrival, and as a crosswind during the final approach. It is therefore referred to as tail wind profile in the following discussions. The hypothetical head wind profile had the same wind speed profile but with the wind directions flipped about the line of longitude at the airport so that it would be experienced as a head wind during most of the arrival and as a crosswind during the final approach. Distributions of the minimum feasible spacing were obtained for each wind profile. The means and standard deviations are shown in Fig. 18. The standard deviations are presented as error bars on top of the mean values.

From Fig. 18, it is seen that the means of the minimum feasible spacing were higher under tail wind and lower under head wind than under zero wind. The sequence-independent target spacing for an average conditional probability of 68.2% were 15, 14.71, and 13.82 for tail wind, zero wind, and head wind, respectively. These results suggest that different target spacing should be used for different wind conditions, especially when the differences in wind speeds are large.

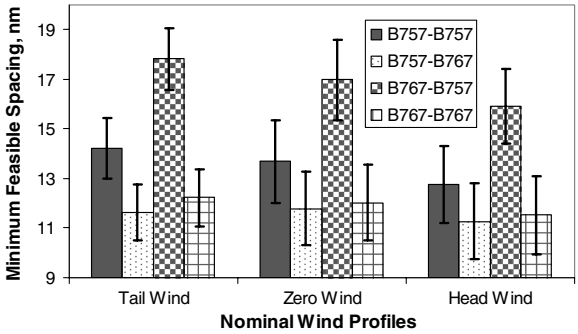

Fig. 18 Effect of the nominal wind profiles.

F. Effect of the Location of the Intermediate Metering Point

The effect of the location of the metering point on target spacing was also studied. To this end, the distributions of the minimum feasible spacing were determined at three additional waypoints: CHERI (at along-track distance −43.3 nm), a point at along-track distance −34 nm, and a point at along-track distance −25 nm. The distances between points are 9–10 nm. The mean wind profile was used as the nominal wind profile. The means and standard deviations of the minimum feasible spacing for each of the metering points are shown in Fig. 19. It is seen that as the metering point moved closer to the runway, both the means and the standard deviations became smaller. The averages of the means and standard deviations were 13.97/1.18, 12.69/1.06, 10.03/0.81, and 9.06/0.57 nm at SACKO, CHERI, −34 nm, and −25 nm respectively.

To determine the impact of metering point location on throughput, a sequence-independent target spacing was obtained for the conditional probability of 68.2% at each of the four points. The resulting final separation buffer and throughput for each target spacing are listed in Table 6. As seen from the table, the target spacing to achieve the same average conditional probability became smaller as the metering point moved closer to the runway threshold. The target spacing was reduced from 15 nm at SACKO to 9.41 nm at 25 nm from runway threshold. At the same time, the throughput increased as the metering point moved closer to the runway threshold; from 29.62 at SACKO to 30.73 at 25 nm from the runway threshold.

Aside from reducing the target spacing and increasing the theoretical throughput, a metering point closer to the runway threshold would give controllers more time and airspace to adjust the spacing between aircraft. Thus, it is reasonable to expect that the adjusted traffic distribution (similar to that shown in Fig. 17) would have a narrower variation and higher percentage satisfying the target spacing at a metering point that is closer to the runway. This in turn would give an even higher total probability for the same average conditional probability.

This analysis suggests that, for a given procedure, target spacing could be provided at optional metering points along the RNAV flight path to allow for operational flexibility in accommodating different traffic loads. At lower traffic densities, metering points farther away from the airport could be used to allow more fuel and time savings per flight. At higher traffic densities, metering points closer to the runway threshold could be used to allow more flights to perform RNAV procedures, albeit starting at a lower altitude.

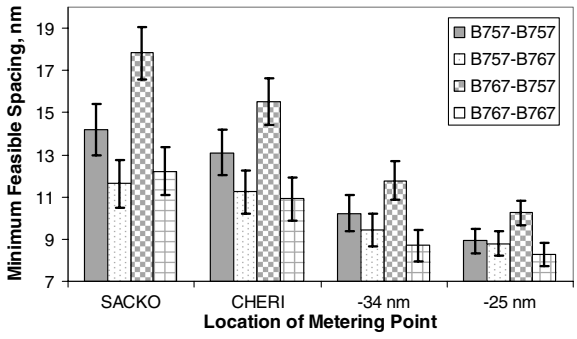

Fig. 19 Effect of the locations of metering point.

Table 6 Final separation buffer and throughput for average conditional probability of 68.2%

Metering Point		SACKO	CHERI	−34 nm	−25 nm
S_I[a]		15	13.69	10.65	9.41
B757–B757	β_{fi}[a]	0.27	0.21	0.19	0.26
	C_i	30.40	30.70	31.00	30.73
B757–B767	β_{fi}	1.25	0.96	0.58	0.34
	C_i	28.88	28.55	29.25	30.73
B767–B757	β_{fi}	−0.94	−0.66	−0.46	−0.46
	C_i	30.40	30.70	31.00	30.73
B767–B767	β_{fi}	1.02	1.10	0.95	0.62
	C_i	28.88	28.55	29.25	30.73
Average	β_f	0.40	0.40	0.31	0.19
	C	29.62	29.60	30.10	30.73

[a]S_I and β are in nm.

G. Separation Analysis Accuracy

The accuracy of separation analysis, the accuracy of target spacing for given desired probabilities, is determined by the accuracy of the PDFs of minimum feasible spacing. Because no specific distribution model has been assumed in the analysis, the accuracy of the PDFs is determined by the data itself, that is, the sample size, and the source of data. Should radar data be used, the number of flight trajectory pairs available for analysis becomes the only factor. Should flight simulation data be used, as presented in this section, the number of trajectory pairs is usually not an issue. Modeling accuracy becomes the factor. With the carefully developed Monte Carlo simulation tool (see Sec. IV), the simulation results matched the KSDF flight test data well [17]. On the other hand, data collected from flight test and operations can be used to calibrate the model components and thus further improve simulation accuracy.

VI. Conclusions

The theoretical framework and the separation analysis methodology presented in this paper may be used to determine, to a desired probability, the target spacing at a selected metering point that will allow a pair of aircraft to perform Area Navigation arrivals without further controller intervention. The methodology uses aircraft trajectories from radar tracks or simulated trajectories. In the accompanying Monte-Carlo-based aircraft trajectory simulation tool that has been developed to support the application of this methodology, various uncertainty factors such as pilot actions, aircraft landing weight, and winds are modeled to provide accurate and reliable estimates of aircraft trajectory variations. Based on the results of the numeric simulation and separation analyses that were conducted for a hypothetical Area Navigation arrival to KSDF, we have concluded the following:

1) The conditional probability method is a useful way to determine target spacing because it directly connects target spacing at the metering point to conditional probability. Thus, the analysis results can be easily visualized to support the design of Area Navigation arrivals.

2) The total probability method gives more realistic estimates of the probability for the given target spacing. Additionally, it can be used to evaluate the feasibility of an Area Navigation arrival under given traffic conditions, and to determine the target spacings that best fit the given traffic conditions. However, it takes additional effort to obtain the data required to generate the PDFs of the actual traffic spacings. If such data are not readily available, controller-in-the-loop simulation studies could be used to collect these data. With sufficient radar data or simulation data, a generic model for the actual traffic at a specific metering point may be developed as a function of the mean of unadjusted traffic spacing, the standard deviation of unadjusted traffic spacing, and the target spacing.

3) There are significant benefits to using sequence-specific target spacings relative to the current practice of using a single miles-in-tail restriction or target spacing. However, the use of multiple target spacings increases the number of variables that controllers must use because the number of aircraft sequences is proportional to the square of the number of aircraft types in the arrival stream. Sequence-specific target spacings will need to be consolidated to keep the number of variables within a manageable level.

4) The current practice of giving miles-in-trail restrictions in increments of 5 nm is not efficient, as the computed target spacing are not integer multiples of 5 nm. Thus, it is necessary to reduce the discretization increment step from 5 nm to a smaller number.

5) Winds have a strong impact on the minimum feasible spacing. If efficiency is a big concern, such as in relatively busy terminal areas or during relatively busy times of the day, different sets of target spacing should be developed for different wind conditions. In this case, a strong tail wind condition would need larger target spacings, and a strong head wind condition would need smaller target spacings.

6) For the same conditional probability, traffic throughput will be significantly improved as the metering point is moved closer to the runway threshold.

The tradeoff optimization problems formulated in this paper can be solved to determine different sets of target spacings for combined scenarios with different wind conditions, traffic mix, and traffic load to allow for as many as possible aircraft to perform uninterrupted Area Navigation arrivals within the manageable limit at relatively high traffic level.

Although we have focused on the case of a single stream of aircraft, the separation analysis methodology can also be applied to merging streams (from different entry points) destined to the same runway. In the case of merging streams, the target spacing problem becomes a traffic coordination problem. Two new elements associated with winds come into play. The first is the nominal wind profiles. Given the same nominal wind profile, the headwind and crosswind components will be different for different streams due to differences in their lateral paths. The other is the wind profile difference between flights on the paths. Aside from the influence of winds, aircraft trajectories in terms of distance vs time will have systematic differences on different lateral paths, mainly due to differences in procedure parameters. Aircraft pairs will have to be categorized by sequence and path rather than by sequence only. However, the principle of the separation analysis presented in this paper is still applicable. Instead of spacing at the metering point between a pair of consecutive aircraft on the same path, distances of the "trailing" aircraft to its metering point, measured at the time when the "leading" aircraft on the other path is at its metering point, can be used for the analysis. The analysis could even be more straightforward if it is based on time of arrival at the metering point for each path.

Acknowledgments

Portions of the work presented here were funded by the FAA under the PARTNER project "Continuous Descent Approach" and NASA under project "Advanced Noise Abatement Procedures for Approach," NAG2-1554. The authors would like to thank Kevin Elmer, Kwok-On Tong, and Joseph K. Wat of Boeing; Nhut Ho of California State University Northridge; Dannie Bennett, Sarah Johnson, David Senechal, and Andrew Willgruber of FAA; David Williams of NASA; and Jeffery Firth, Robert Hilb, Stuart Lau, and James Walton of UPS for sharing their valuable expertise in helping us to develop various components of the aircraft simulator. Thanks also to Frank M. Cardullo of SUNY Binghamton, Eric Feron of GaTech, and Charles M. Oman of Massachusetts Institute of Technology for their valuable suggestions.

References

[1] Robinson, S. M., DeArmon, J. S., and Becher, T. A., "Benefits of RNAV Terminal Procedures: Air/Ground Communication Reduction and Airport Capacity Improvements," *Proceedings: The 21st Digital Avionics Systems Conference (21st DASC)*, Vol. 1, IEEE, Piscataway, NJ, Oct. 2002, pp. 2.D.1-1–11.

[2] Sprong, K. R., Haltli, B. M., DeArmon, J. S., and Bradley, S., "Improving Flight Efficiency Through Terminal Area RNAV," FAA/EUROCONTROL Paper 7, June 2005.

[3] Clarke, J.-P. B., Ho, N. T., Ren, L., Brown, J. A., Elmer, K. R., Tong, K.-O., and Wat, J. K., "Continuous Descent Approach: Design and Flight Test for Louisville International Airport," *Journal of Aircraft*, Vol. 41, No. 5, 2004, pp. 1054–1066.

[4] Lee, J. J., "Modeling Aviation's Global Emissions, Uncertainty Analysis, and Applications to Policy," Ph.D. Thesis, Dept. of Aeronautics and Astronautics, Massachusetts Institute of Technology, Cambridge, MA, 2005.

[5] Clarke, J.-P., Bennett, D., Elmer, K., Firth, J., Hilb, R., Ho, N., Johnson, S., Lau, S., Ren, L., Senechal, D., Sizov, N., Slattery, R., Tong, K., Walton, J., Willgruber, A., and Williams, D., "Development, Design, and Flight Test Evaluation of a Continuous Descent Approach Procedure for Nighttime Operation at Louisville International Airport," PARTNER CDA Development Team, Report No. PARTNER-COE-2006-02, Cambridge, MA, Jan. 2006.

[6] *Update to Roadmap for Performance-Based Navigation—Evolution for Area Navigation (RNAV) and Required Navigation Performance (RNP) Capabilities 2006–2025*, FAA, Washington, DC, 2006.

[7] Laqui, C., Barker, D. R., DeArmon, J. S., and Farrell, D. W., "Terminal RNAV: Analyses of Las Vegas McCarran International Airport Terminal RNAV Operations," *Proceedings: the 22nd Digital Avionics Systems Conference (22nd DASC)*, Vol. 1, IEEE, Piscataway, NJ, Oct. 2003, pp. 1.E.2-1–11.

[8] Weitz, L. A., Hurtado, J. E., and Bussink, F. J. L., "Increasing Runway Capacity for Continuous Descent Approaches Through Airborne Precision Spacing," AIAA Paper 2005-6142, Aug. 2005.

[9] Becher, T. A., Barker, D. R., and Smith, A. P., "Methods for Maintaining Benefits for Merging Aircraft on Terminal RNAV Routes," *Proceedings: the 23rd Digital Avionics Systems Conference (23rd DASC)*, Vol. 1, IEEE, Piscataway, NJ, Oct. 2004, pp. 2.E.1-1–13.

[10] Barker, D. R., Haltli, B. M., Laqui, C., MacWilliams, P., and McKee, K. L., "Assessment of Terminal RNAV Mixed Equipage," *Proceedings: the 23rd Digital Avionics Systems Conference (23rd DASC)*, Vol. 1, IEEE, Piscataway, NJ, Oct. 2004, pp. 2.B.2-1–13.

[11] Becher, T. A., Barker, D. R., and Smith, A. P., "Near-Term Solution for Efficient Merging of Aircraft on Uncoordinated Terminal RNAV Routes," *Proceedings: the 24th Digital Avionics Systems Conference (24th DASC)*, Vol. 1, IEEE, Piscataway, NJ, Oct.–Nov. 2005, pp. 2.D.3-1–12.

[12] "Air Traffic Control," FAA Order 7110.65R, Washington, DC, Feb. 2006, pp. 5-5-2–5-5-3.

[13] *Aeronautical Information Manual—Official Guide to Basic Flight Information and ATC Procedures*, FAA, Washington, DC, Feb. 2006, pp. 4-4-7,7-3-7–7-3-8.

[14] Ren, L., Clarke, J.-P. B., and Ho, N. T., "Achieving Low Approach Noise Without Sacrificing Capacity," *Proceedings: the 22nd Digital Avionics Systems Conference (22nd DASC)*, Vol. 1, IEEE, Piscataway, NJ, Oct. 2003, pp. 1.E.3-1–9.

[15] Kopardekar, P., Green, S., Roherty, T., and Aston, J., "Miles-In-Trail Operations: A Perspective," AIAA Paper 2003-6700, Nov. 2003.

[16] Ren, L., Ho, N. T., and Clarke, J.-P. B., "Workstation Based Fast-Time Aircraft Simulator for Noise Abatement Approach Procedure Study," AIAA Paper 2004-6503, Sept. 2004.

[17] Ren, L., "Modeling and Managing Separation for Noise Abatement Arrival Procedures," Sc.D. Thesis, Dept. of Aeronautics and Astronautics, Massachusetts Institute of Technology, Cambridge, MA, Sept. 2006.

[18] "United States Standard for Required Navigation Performance (RNP) Approach Procedures with Special Aircraft and Aircrew Authorization Required (SAAAR)," FAA Order 8260.52, Washington, DC, June 2005, pp. 2-7–2-8.

[19] *UPS B757/767 Aircraft Operating Manual*, Document: UPS33075, UPS Flight Publications, Louisville, KY, 2003.

[20] Ho, N. T., and Clarke, J.-P. B., "Mitigating Operational Aircraft Noise Impact by Leveraging on Automation Capability," AIAA Paper 2001-5239, 2001.

[21] "NOAA/ESRL/GSD Aircraft Data Web," [online database], http://acweb.fsl.noaa.gov/ [retrieved 5 Aug. 2006].

[22] Ren, L., and Clarke, J.-P. B., "Development and Application of Separation Analysis Methodology for Noise Abatement Approach Procedures," AIAA Paper 2005-7397, Sept. 2005.

[23] Larson, R. C., and Odoni, A. R., *Urban Operations Research*, Prentice–Hall, Englewood Cliffs, NJ, 1981, pp. 48–49.